IEEE Access
Multidisciplinary | Rapid Review | Open Access Journal

Received April 30, 2020, accepted May 14, 2020, date of publication May 19, 2020, date of current version June 2, 2020.

Digital Object Identifier 10.1109/ACCESS.2020.2995591

Design and Analysis of Tension Control System for Transformer Insulation Layer Winding

HAIXIANG HUANG[1], JIAZHONG XU[1], KEWEI SUN[2], LIWEI DENG[1], AND CHENG HUANG[1]
[1]School of Automation, Harbin University of Science and Technology, Harbin 150080, China
[2]School of Mechanical Engineering, Harbin University of Science and Technology, Harbin 150080, China

Corresponding author: Jiazhong Xu (xujiazhong@126.com)

This work was supported in part by the Research and Development and Cultivation Projects of Scientific and Technological Achievements of Provincial Universities in the Department of Education of Heilongjiang Province under Grant TSTAU-R2018002, and in part by the Natural Science Foundation of Heilongjiang Province under Grant LH2019F024.

ABSTRACT The insulation performance of the core transformer is determined by the winding quality of the insulation layer between the coils. It is necessary to assure uniform winding tension in order to ensure the insulation performance of the transformer and improve production efficiency. Thus, in this article, the dynamic characteristics of the transformer insulation winding process are analyzed, and the insulation winding tension control system is designed to decrease the tension fluctuation caused by the alternating change of the elliptical core radius in the winding process. Firstly, the time-varying characteristics of roll radius and inertia are analyzed, the mechanical structure and dynamic models of unwinding and rewinding are established, and the effects of upstream and downstream span length and dancer inertia on the resonant frequency and response performance of the system are revealed. Later, the influence factors of tension fluctuation and disturbance propagation frequency are investigated, and the tension control model of Hybrid dancer position feedback is established. The variable universe fuzzy PI controller is designed by setting fuzzy rules and universe adjustment factors. Finally, the stability of the controller and the weakening effect on the tension disturbance are verified by simulation, and the performance and application value of the automatic winding tension control system are tested by a series of experiments.

INDEX TERMS Transformer insulation winding, tension control, disturbance, variable universe fuzzy PI, hybrid dancer.

I. INTRODUCTION

The transformer, as the basic equipment for power transmission and transformation, is widely used in power plants, converter stations, and substations. It occupies a pivotal position in the power industry and is also the basic components for industrial transformation. Its demand is increasing with each passing day, and the market prospect is very broad. The winding machine is one of the key equipment in transformer production. With the development of automatic winding technology, an automatic winding machine with high efficiency, low production cost, compact coil, and high filling coefficient has been widely used in transformer production [1], [2].

Coil winding is the core process of transformer manufacturing, which not only determines the mechanical, insulation, and heat resistance performance of the transformer but also affects the economic indicators of the transformer [3]. It is necessary to add an insulation layer between the winding layers to ensure the insulation performance of the transformer and reduce the risk of voltage flashover of adjacent winding layers. The traditional placement of transformer interlayer insulation requires workers to cut the surface insulation according to the size of the transformer core and then cover the wide paper sheet on the winding surface. The placement of end insulation is that workers stick the thick insulation strips stacked by multiple layers to both ends of the transformer core mold. As shown in Fig 1 (a), the tension control in the winding process depends on the experience and proficiency of workers. The insulation layer is the part that consumes the longest working time and has the lowest efficiency in the winding process of the transformer.

Using the idea of continuous winding of thin strip insulation tape instead of wide strip insulation layer covering, the automatic insulation layer winding system of transformer

The associate editor coordinating the review of this manuscript and approving it for publication was Padmanabh Thakur.

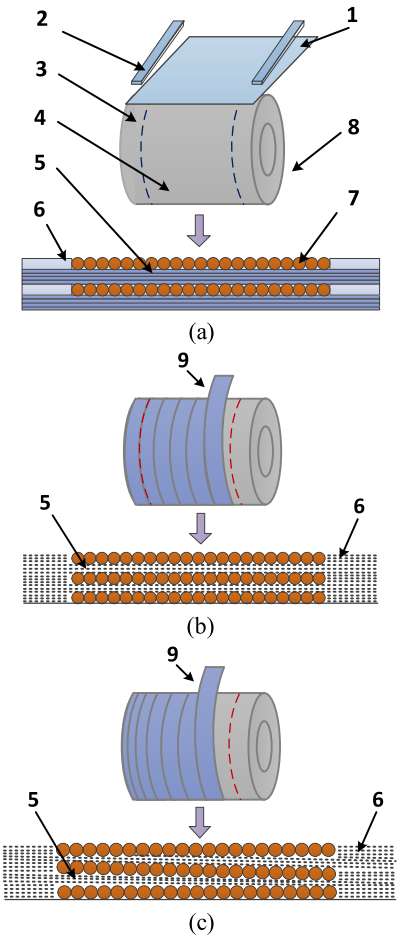

FIGURE 1. Schematic diagram of a traditional winding method and continuous winding of the insulating tape: 1-Insulation web 2-Thick insulation strip 3-End insulation area 4-Interlayer insulation area 5-Interlayer insulation 6-End insulation 7-Copper wire 8-Transformer core mold 9-Insulation tape. (a) Traditional winding. (b) Equal spacing winding. (c) Gradient winding.

winding machine can solve the complicated labor of workers, and the equal-spacing and gradient winding of insulation tape can be realized in the winding process [4], as shown in Fig 1 (b) and (c). The core technology of insulation tape tension control in the winding process mainly depends on the design of the tension control system. In order to improve and enhance the performance of the tension control system, researchers have done much in-depth research. Industrial tension control systems usually use PI controllers with fixed gains [5]–[7]. This requires setting the gain according to the working environment and material parameters. Due to changes in operating conditions and web parameters, and uncertainty in the system, leading to this is a difficult task. The fixed PI gain cannot well meet the changing needs of the system state and even cause the system to be unstable in some cases. T Nishida *et al.* constructed a self-correcting PI controller with an estimator based on an adaptive particle swarm algorithm [8]. Pramod R *et al.* used model-based reference and relay feedback methods to design adaptive PI controllers [9]. In order to effectively reduce and compensate for the tension disturbance existing in the system, S H Liu *et al.* designed an auto-disturbance-rejection controller to improve the stability of the system [10]. As the speed difference between the two axes can cause obvious tension disturbances in the system, to reduce the synchronization speed error between the two axial systems, aiming at the uncertain model of transformer winding system, Van Tu Duong *et al.* proposed a cross-coupling synchronous speed control method based on model reference adaptive [11]. Adding a tension sensor to the system, direct feedback of the tension can be achieved; however, an observer-based tension control strategy can be used to avoid measurement errors caused by insufficient accuracy and reduce the cost and complexity of the control system. The presence of disturbances is well observed [12]–[14]. In order to improve the robustness of the tension control system and meet the requirements of tension control for real-time performance and response speed, Vincent Gassmann *et al.* proposed an improvement method based on H∞[15].

Many factors need to be considered in the design of the tension control system, and the slight change of speed can cause obvious fluctuation of tension. This paper needs to realize the automatic winding of the insulation layer of the oval iron core transformer. The geometric shape of the winding core shaft, besides the acceleration and deceleration process, can affect the large fluctuation of tension. During the insulation belt transmission from unwinder to the main shaft, for example, in the process of fixation under constant torque, the tension of the insulating tape can change with the radius change of the unwinder and the transformer core mold [16], [17]. If the tension is too small, the main shaft cannot drive the insulating belt forward, resulting in relaxation that will affect the tightness of the next layer of the coil. If the tension is too large or suddenly increased, in addition to wasting torque, it will also cause deformation or even damage to the insulating belt. To obtain better winding quality, it is essential to keep the uniform tension of the insulating belt, and the passive dancer mechanism, which is composed of springs, shock absorbers, and rollers, has the function of energy storage that may attenuate the impact on the system when the speed and tension change suddenly [18]. The active dancer mechanism has an external driver. By measuring the position of the roller, the external actuator forces the roller to adjust the tension, which has the function of feedback tension [19]. This paper, thus, combines the two to design a hybrid dancer mechanism for tension and speed degree disturbance buffer. The design of the variable universe fuzzy controller does not need much experience of experts in relevant fields but only needs to know the general trend of rules. Since its universe is adjusted in time with the change of error equivalent to adding fuzzy rules, the universe division and the membership function selection turns out to be the less significant factors [20], [21], also enhancing the fault-tolerant ability of system control. According to the above analysis, aiming at the problems of low efficiency of insulating layer

placement, as well as poor product quality and consistency, a fuzzy PI tension control system with hybrid dancer position feedback is suggested in this study for transformer insulating layer automatic winding, which realizes automatic and efficient winding of insulating layer, stabilizes the tension in the winding process, and decreases the tension disturbance caused by the spindle geometry.

This paper is organized as follows: In the second section, the automatic winding system of the insulation layer is offered, and the dynamic model is developed. In the third section, the causes of the tension disturbance are analyzed, the frequency of the disturbance is predicted, the tension control strategy is presented, and the tension controller based on a fuzzy theory of the variable universe is designed. In the fourth section, the controller is simulated and tested using experiments, and the performance of the proposed tension control system is verified as compared to the traditional PID control method.

II. MECHANICAL STRUCTURE AND DYNAMIC MODELING

Fig 2 is a schematic diagram of the designed automatic winding system for the insulation layer of the transformer. The entire system is divided roughly into three sections, the unwinding section, the transportation section, the rewinding section; the rewinding is the main shaft that primarily realizes speed adjustment. The insulating tape is installed on the mandrel of the unwinder, and a certain initial speed ratio exists between the main and the uncoiling shaft, causing continuous tension in the winding process. The tension adjustment is to adjust the pressure in the dancer cylinder by the potentiometer knob of the control panel. If the dancer arm remains in the reference position during the system operation, the cylinder pressure on the dancer arm is approximately equal to twice the tension setting value (the gravity action of the dancer itself and the insulating tape need to be considered; thus, generally, the cylinder pressure is slightly more than twice the expected tension value). Therefore, a displacement sensor is added to the dancer part. The unwinder speed is adjusted by position feedback so that the dancer may be kept near the reference position as far as possible, and the continuous tracking of tension may be realized. The dynamic

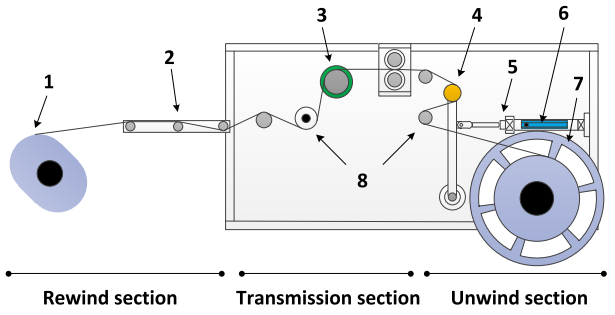

FIGURE 2. Schematic diagram of transformer insulation tape automatic winding system: 1-Rewind roll 2-Guide roll 3-Counting roll 4-Dancer roll 5-Cyliner 6-Position sensor 7-Unwind roll 8-Guide roll.

characteristics of free rollers are typically overlooked since they only affect the dynamic characteristics of the system throughout acceleration and deceleration. In the present research, it is supposed that there is no relative slip, in the process of transmission, between the paper tape and the roller. The analysis of the dynamic characteristics of the unwinding and rewinding section is as the following.

A. UNWIND ROLL MODELING

The unwind section includes the unwinder and the dancer mechanism. A servo motor gives rise to the unwinding shaft. As the winding task progresses, the radius of the insulating paper tape reel on the unwinding roller continuously reduces. The effective moment of inertia J_1 (t) at time t may be expressed as:

$$J_1(t) = J_{m1} + J_{c1} + J_{w1}(t) \tag{1}$$

where J_{m1} is the inertia of all rotating components on the motor side, J_{c1} is the inertia of uncoiling roller, and J_{w1} (t) is the inertia of insulated paper tape reel and material. J_{m1} and J_{c1} are constants that do not change with time. Owing to the constant transmission of insulating paper tape, J_{w1} (t) changes over time. J_{w1} (t) may be expressed as:

$$J_{w1}(t) = \frac{\pi}{2} Hp(R_1^4(t) - R_{c1}^4(t)) \tag{2}$$

where H is the width of insulating paper tape, p is the density of insulating paper tape, R_{c1} is the radius of uncoiling roller, and R_1(t) is the radius of insulating paper tape reel. The dynamic model of the uncoiling roller may be defined as follows:

$$\dot{J}_1 w_1 + J_1 \dot{w}_1 = T_1 R_1 - n_1^2 U_1 - b_{f1} w_1 \tag{3}$$

where n_1 is the transmission ratio between the servo motor shaft and the uncoiling roller, w_1 is the angular speed of the uncoiling roller, and b_{f1} is the friction coefficient of the uncoiling roller. From formula (1), it may be concluded that the rate of change of J_1 (t) is only associated with J_{w1} (t), and the rate of change of J_1 (t) can be obtained from formula (2) as follows:

$$\dot{J}_1(t) = \dot{J}_{w1}(t) = 2\pi Hp R_1^3 \dot{R}_1 \tag{4}$$

The change rate $\dot{R}_1$ of R_1 is a function of the tangent speed of V_1 the insulating tape and the thickness w of the insulating tape that may be defined as follows:

$$\dot{R}_1 \approx -\frac{wV_1(t)}{2\pi R_1(t)} \tag{5}$$

$\dot{R}_1$ in formula (5) is an approximate representation since the radius only changes when the tape winding is completed. The tangential velocity V_1(t) of t at any time is associated with the angular velocity w_1(t) of the uncoiling roller and the radius of the insulating tape at that time; thus, it may be achieved:

$$\dot{w}_1 = \frac{\dot{V}_1}{R_1} - \frac{\dot{R}_1 V_1}{R_1^2} \tag{6}$$

According to formulas (3), (4), (5), and (6), the following can be obtained:

$$\frac{J_1}{R_1}\dot{V}_1 = T_1R_1 - n_1^2U_1 - b_{f1}\frac{V_1}{R_1} - \frac{w}{2\pi R_1}\left(\frac{J_1}{R_1^2} - 2\pi HpR_1^2\right)V_1^2 \tag{7}$$

The insulating paper tape with a span between uncoiling roller and dancer roller is analyzed by using the law of mass conservation, and the dynamic characteristics of uncoiling roller tension T_1 are given by the following formula:

$$L_1\dot{T}_1 = AE\,(V_2 - V_1) + V_1T_0 - V_2T_1 + AEl_d\dot{\theta}(t) \tag{8}$$

where L_1 is the length of the insulating paper tape between the uncoiling roller and the dancer roller, A is the cross-sectional area of the insulating paper tape, E is Young's elastic modulus of the insulating paper tape, V_2 is the speed of the dancer roll, T_0 is the entrainment tension of the insulating paper tape on the uncoiling roll, l_d is the length of the dancer swing arm, and θ is the offset angle of the dancer. In the working process of the uncoiling rod, the radius and inertia are reducing, and the dynamic characteristics of the system are continuously changing. Under the assumption that the radius change is quasi-static, the gain constant between the control signal and the tension of the insulating paper tape is approximately proportional to the inverse of the radius, $\mathrm{Gain_U}\left(\frac{T_u}{u_u}\right) = \frac{1}{R_u}$; if there is a large difference in inertia in the actual system, it will decrease the performance of the controller and even lead to system instability. It is, therefore, essential to compute the moment of inertia of the uncoiling part and the radius of the uncoiling roller in real time and accurately in the unwinding control process. They are added to the feedforward control signal to take part in tension control to decrease tension fluctuations. The feedforward compensation controller has been designed in reference [12], [13].

On the basis of the approximate Archimedes helix length, the approximate length of the insulating tape conveyed from the unwinder may be achieved as follows:

$$L_{web} = \pi n_{winder}(2R_0 - n_{winder}H) \tag{9}$$

$$H = \frac{2\pi n_{winder}R_0 - L_{web}}{\pi n_{winder}^2} \tag{10}$$

where n_{winder} is the total number of rotation of the uncoiling roller, and R_0 is the initial radius of the insulating paper tape on the uncoiling roller. To estimate the radius efficiently, L_{web} and n_{winder} can integrate V_1 and $\frac{\omega}{2\pi H}$, respectively.

$$R_{est} = R_0 - wn_{winder} = \frac{L_{web}}{\pi n_{winder}} - R_0 \tag{11}$$

Combining the radius of the current unwinding roll and the initial parameters entered may efficiently calculate the moment of inertia. The initial parameters entered comprise the mass and radius of the roll and the hollow core drum, together with the inertia and transmission ratio of the unchanged part of the equipment. According to the calculation of the radius of the insulating paper tape on the reeling roller, the approximate quality of the paper tape on the roll may be achieved initially:

$$m_{web_{est}} = \rho_{web}\pi\left(R_{est}^2 - R_{core}^2\right) \tag{12}$$

$$J_{web_{est}} = \frac{1}{2}m_{web_{est}}\left(R_{est}^2 - R_{core}^2\right) \tag{13}$$

The density of insulating paper tape per meter length of the reel may be defined as:

$$\rho_{web} = \frac{m_{full} - m_{core}}{\pi\left(R_{full}^2 - R_{core}^2\right)} \tag{14}$$

Therefore, formula (11) can be expressed as:

$$J_{web_{est}} = \frac{1}{2}\frac{\left(m_{full} - m_{core}\right)\left(R_{est}^4 - R_{core}^4\right)}{R_{full}^2 - R_{core}^2} \tag{15}$$

For the inertia of the whole system, the insulating tape, reel, and roll are essential to be calculated to the motor side.

$$J_{total} = J_{sys} + \frac{J_{core} + J_{web_{est}}}{N^2} \tag{16}$$

B. DYNAMIC ANALYSIS OF DANCER MECHANISM

The hybrid dancer system is shown in Fig 3. The angular displacement dynamic characteristics of dancer are obtained based on torque balance, which can be expressed as follows:

$$J_d\frac{d^2\theta}{dt^2} = F_cl_c\cos\theta - (l_d - R_2)\,T_1\cos\theta - M_dgl_g\sin\theta - B_f - (l_d + R_2)\,T_2\cos\theta \tag{17}$$

where J_d and M_d are the inertia and mass of the whole dancer mechanism, F_c is the pressure of the cylinder to the dancer mechanism, l_c is the distance from the fixed center of the dancer pendulum circle to the cylinder, T_1 and T_2 are the upstream and downstream tension of the dancer, and R_2 is the radius of the dancer roller. Since the spindle mandrel is non-circular, the angular displacement θ of the dancer is always floating, and the floating of the dancer is larger in the acceleration and deceleration stage that may efficiently reduce the impact on the system due to the sudden change of velocity.

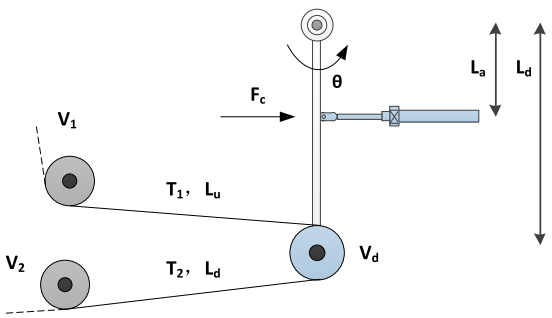

FIGURE 3. Dancer subsystem model.

The cylinder support force for the dancer to keep the dancer in the reference position in the steady-state:

$$F_c = \frac{2L_d T_{ref}}{L_a} \tag{18}$$

where L_d is the distance from the center of the circle around the dancer arm to the center of the dancer roll, L_a is the distance from the center of the circle around the dancer arm to the support point of the cylinder, and T_{ref} is the expected tension.

By changing the span length of the upstream and downstream and the inertia of the dancer system, their influence on the resonant frequency and response performance of the system is analyzed and mastered. Figs 4 and 5 demonstrate the bode diagram.

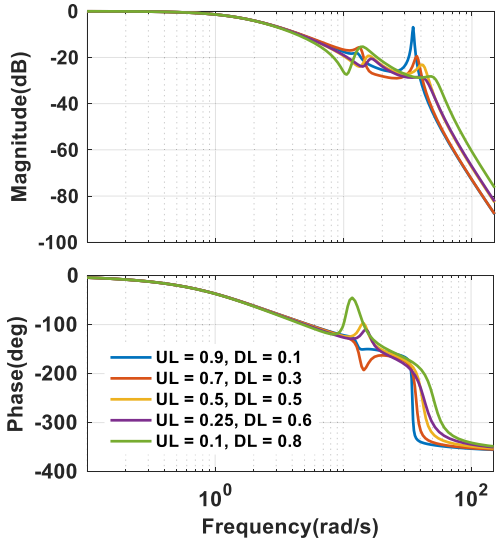

FIGURE 4. Bode plots with different span lengths.

By the increase of the downstream span, the resonant frequency increases, and the bandwidth widens. Shortening the upstream span and increasing the downstream span, thus, make the former smaller than the latter, which may efficiently improve the stability and responsibility of the hybrid dancer system. The smaller the inertia of the dancer mechanism, the higher the resonant frequency. When designing the dancer mechanism, decreasing its inertia can moderately improve the control performance of large-scale interference. In the design of the hybrid dancer tension control system, it is essential to achieve a shorter upstream span and less dancer inertia so that the system can maintain a good response even at low operating speed, and the PI gain determined at low speed can also meet the requirements of high-speed operation.

C. REWIND ROLL MODELING

In spindle winding process, the spindle radius R_3 becomes larger, and the inertia J_3 increases; the dynamics of the spindle part is similar to that of the unwinding part that may be

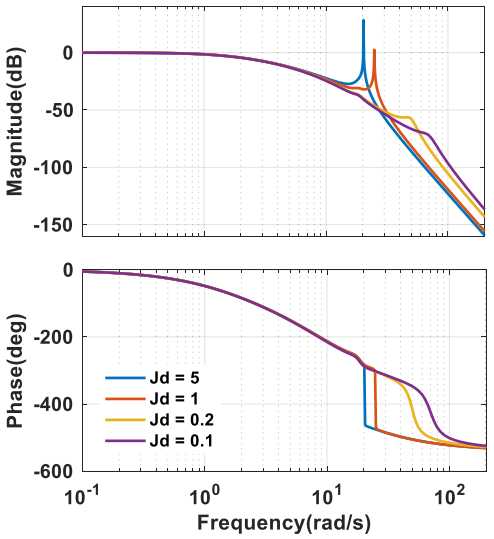

FIGURE 5. Dancer bode plot with different inertia.

expressed as follows:

$$\frac{J_3}{R_3}\dot{V}_3 = -T_2R_3 + n_3^2U_3 - b_{f3}\frac{V_3}{R_3} - \frac{w}{2\pi R_3}\left(\frac{J_3}{R_3^2} - 2\pi HpR_3^2\right)V_3^2 \tag{19}$$

$$L_2\dot{T}_2 = AE\,(V_3 - V_2) + V_2T_1 - V_3T_2 + AEl_d\dot{\theta}(t) \tag{20}$$

III. CONTROLLER DESIGN

When the PI control method after setting gain is used to wind the insulation layer of transformer, the change curve of tension and dancer position of the unwind section is as shown in figure 6, the reference tension is 50N, the dancer position and tension overshoot when the unwinder accelerates and decelerates, and the tension has an apparent steady-state error when the speed is at the reference value for a while. It may be observed from the figure that the tension fluctuation is greater than ±6% of the working tension, and the maximum fluctuation exceeds 10% of the reference value. There is a strong coupling between the position of the dancer and the tension and the velocity.

The fundamental reason for the tension disturbance is the continuous change of speed. First, in steady-state operation, due to the geometric shape of the rewinding roll, when it moves to the long side of the roll, the radius smaller, and the tangential velocity decreases, whereas, when it moves to the short side of the roll, the radius becomes larger, and the tangential velocity increases, resulting in a large tension fluctuation. Secondly, owing to the continuous reduction of the radius of the paper tray in the unwinding process, the tangent speed of the tape changes, resulting in tension disturbance, and the tension fluctuation will be transferred to the next stage [22].

Typically, the allowable tension fluctuation is ±4% of the working tension. Therefore, in the controller design process,

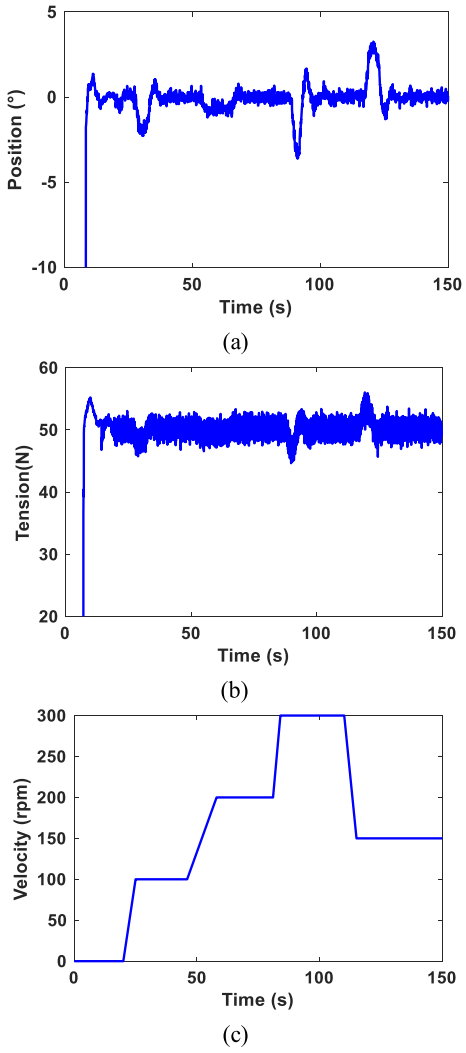

FIGURE 6. Experimental results under the fixed gain PI controller. (a) Dancer position. (b) Unwind tension. (c) Unwind speed.

it is essential to consider the performance of the system's response to the maximum tension disturbance and improve the speed of the system's adjustment to the disturbance in order to reduce the tension fluctuation caused by speed change and improve the accuracy of insulating tape tension control. When the paper tape on the uncoiling roller is transported to the next stage, the diameter of the paper tray decreases, and the frequency of tension increases; the range of tension disturbance can be determined by formula (21). If, for instance, the diameter of the uncoiling roller is 0.5m to 0.2m, the maximum frequency is 66.67rad/s to 116.67rad/s when the speed is 400m/min to 700m/min.

$$\omega_{max} = \frac{2v_0}{D_{min}}, \quad \omega_{min} = \frac{2v_0}{D_{max}} \tag{21}$$

The tension disturbance is transmitted from upstream to downstream. The equivalent disturbance propagation process can be obtained by a dielectric filter determined by the span length and the initial velocity to predict the propagation

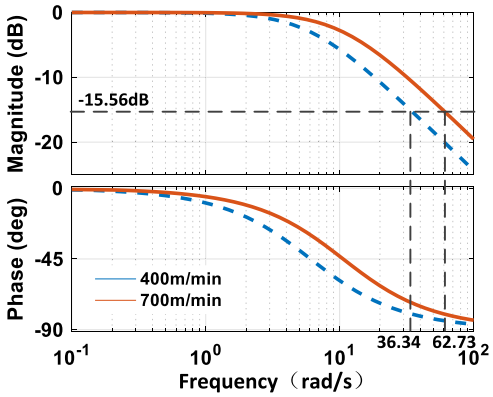

FIGURE 7. Bode diagram of tension disturbance transfer (400 ∼ 700*m*/*min*).

frequency of the tension disturbance in the system. Fig 7 shows the baud diagram determined by formula (22). The maximum disturbance of the uncoiling part is 12N, and the span is 1.1m. When the working speed is from 400m/min to 700m/min, the corresponding amplitude of the disturbance from 12N to 2N is −15.56dB, and the frequencies are 36.34rad/s and 62.72rad/s, respectively. When the disturbance frequency is not lower than 2N, 62.72rad/s can make it less than 2N that meets the working requirements of the system.

$$\frac{T_2(s)}{T_1(s)} = \frac{v_{10}}{Ls + v_{20}}, \quad \left|\frac{T_{op}}{T_1(s)}\right| = \left|\frac{v_{10}}{Ls + v_{20}}\right|_{s=j\omega_{max}} \tag{22}$$

Although PID control is extensively applied in the industry as a classical control method, it cannot effectively adjust the increase of tension interference when used to control the tension of insulating layer winding of oval iron core transformer. In some cases, the disturbance is beyond the normal working range since the tension control system shows a strong nonlinearity, coupling, and uncertainty. The conventional PID control method may only achieve a normal control effect in the local working area of the system, and the control parameters cannot be adjusted in real time with the change of the system dynamic characteristics.

A. VARIABLE UNIVERSE FUZZY PI TENSION CONTROL SYSTEM

Although the traditional fuzzy PID may be adjusted in real time, it hinges on too much on the control rules, and the rules themselves have redundancy and roughness. The performance of the controller is limited by the fixed fuzzy universe and scale factor. Once the input error is reduced, more fuzzy rules fail, leading to large static errors in the control process that cannot meet the needs of control accuracy and adjustment range. The design idea of fuzzy controller based on the variable universe is to change the initial range of input and output domain in real time with the error and error rate of change that may effectively compress the universe when the system error is small, improve the response speed, control accuracy

without increasing the number of control rules, and slightly extend the universe when the error is large in order to adapt to the uncertain disturbance in the system. By introducing the scaling factor to adjust the initial universe scope in real time, the controller adjusts the PI parameters on-line and realizes the variable universe fuzzy PI control. It is essential, in the process of practical application, to multiply all the points in the universe by the scaling factor to simplify the calculation and strengthen the application in order to apply the method of equivalent processing: the quantization factor K_e of error e and the quantization factor K_{ec} of the error change rate $\dot{e}$ are divided by the corresponding input universe scaling factor $\alpha(e)$, $\alpha\ (e_c)$, respectively; the output quantization factor K_{us} is multiplied by the corresponding output universe scaling factors β_p, β_i. The designed tension adjustment system is displayed in Fig 8. K_2 is a proportional coefficient that depends on the unwinding radius and the gear ratio between the roller and the motor shaft. The control scheme consists of the speed inner ring and the position outer ring; the outer ring adjusts the unwinder speed through position feedback to perform tension control, and Beckhoff driver adjusts the inner loop.

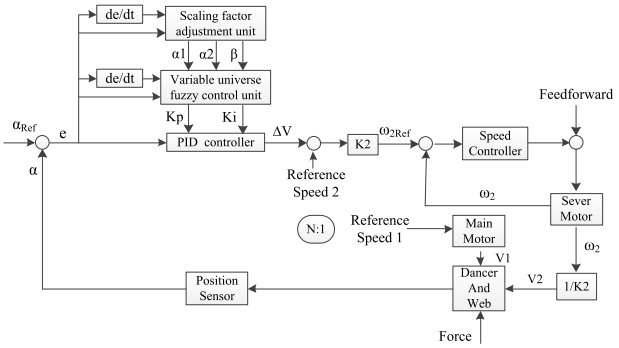

FIGURE 8. Tension control system block diagram.

B. FUZZY PI CONTROLLER

The error e and the rate of error change $\dot{e}$ are applied as the input of the fuzzy controller; ΔK_p and ΔK_i are applied as the output of the controller. The dynamic range of the actual operation of the system is standardized. It is stated that the initial universe of the variables e, ΔK_p, and ΔK_i is $[-6, +6]$, the initial universe of the rate of error change $\dot{e}$ is $[-3, +3]$, and the dynamic range of the actual operation of the system is $[e_{max}, e_{min}]$, $[e_{c_{max}}, e_{c_{min}}]$, $[\Delta K_{s_{max}}, \Delta K_{s_{min}}]$ (wheres = P, I). The standardized transformation formula of the universe is as follows:

$$\begin{cases} K_e = \dfrac{12}{e_{max} - e_{min}}, & E = K_e\left(e - \dfrac{e_{max} - e_{min}}{2}\right) \\ K_{ec} = \dfrac{6}{e_{c_{max}} - e_{c_{min}}}, & E_c = K_{ec}\left(e_c - \dfrac{e_{c_{max}} - e_{c_{min}}}{2}\right) \\ K_{us} = \dfrac{12}{\Delta K_{smax} - \Delta K_{smin}}, & \\ \Delta k_{us} = K_{us}\left(\Delta K_s - \dfrac{\Delta K_{smax} - \Delta K_{smin}}{2}\right) & \end{cases} \tag{23}$$

The fuzzy subset is {NB, NM, NS, ZO, PS, PM, PB}. The S-shaped membership function is used when the language variables are NB and PB, and the triangular membership function is used for other language variables. The membership function of the controller input and output is shown in Fig 9.

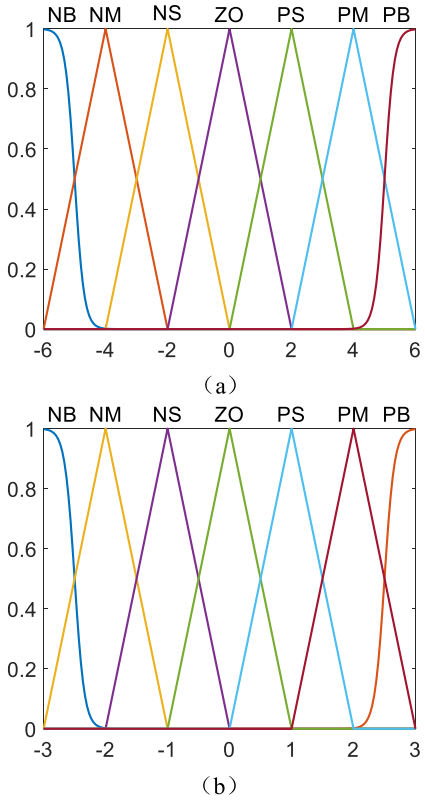

FIGURE 9. Membership function of state variables. (a) e(k). (b) $\Delta e(k)$.

Combined with the experience of tension control expert and PID parameter setting experience, the fuzzy logic rules of tension ΔK_p, ΔK_i are established, as shown in Tables 1 and 2.

TABLE 1. ΔK_p fuzzy logic rules.

Δe/e	NB	NM	NS	ZO	PS	PM	PB
NB	NB	NB	NB	NB	NM	NM	NS
NM	NB	NB	NB	NM	NM	NS	NS
NS	NB	NM	NM	NS	NS	NS	ZO
ZO	NM	NM	NS	NS	ZO	PS	PS
PS	NS	NS	ZO	ZO	PS	PS	PM
PM	PS	PS	PM	PM	PM	PB	PB
PB	PM	PM	PM	PB	PB	PB	PB

The defuzzification output using weighted average is:

$$\Delta k_s = \frac{A_i \sum_i \mu_{(\Delta k_{si})}}{\sum_i \mu_{(\Delta k_{si})}} \tag{24}$$

The output of ΔK_p and ΔK_i in the initial universe is shown in Fig 10.

TABLE 2. ΔK_i fuzzy logic rules.

Δe/e	NB	NM	NS	ZO	PS	PM	PB
NB	NB	NB	NB	NB	NB	NB	NM
NM	NB	NB	NB	NB	NM	NM	NS
NS	NM	NM	NS	NS	NS	ZO	ZO
ZO	NM	NS	ZO	ZO	PS	PS	PM
PS	NS	NS	ZO	PS	PS	PM	PM
PM	PS	PS	PS	PM	PM	PM	PB
PB	PM	PM	PB	PB	PB	PB	PN

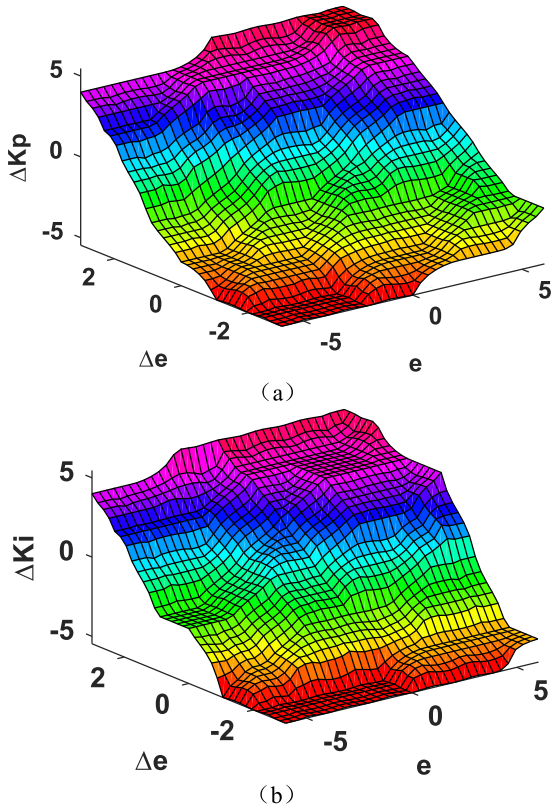

FIGURE 10. Output results of ΔK_P and ΔK_I. (a) Results of ΔK_P. (b) Results of ΔK_I.

Set the parameter adjustment to $K_p = K_{p0}+\Delta K_p$, $K_i = K_{i0}+\Delta K_i$; then, the actual control output of the system is:

$$u(k) = K_p e(k) + K_i \sum_{i=1}^{k} e(i) + K_d e_c(k) \tag{25}$$

C. UNIVERSE ADJUSTMENT FACTOR

The design of the scaling factor can be selected based on fuzzy reasoning or function form. In practical application, the design of the scaling factor is performed in function form to simplify the calculation.

The setting of the input universe scaling factor $\propto_x$ depends only on the input error e and the error rate of change ė, the input universe scaling factor is:

$$\begin{cases} \alpha(x) = \left(\dfrac{|x|}{E}\right)^{\tau} + \varepsilon^{\tau} \\ \alpha(x) = 1 - \lambda exp\left(-kx^2\right) \end{cases} \tag{26}$$

where τ and λ are constants, $0 < \tau < 1$, $0 < \lambda < 1$, and ε is a sufficiently small positive number.

The scaling factor of the input universe is selected as follows: $\alpha(x) = 1 - \lambda exp\left(-kx^2\right)$, where $\lambda = 0.6$, $k = 0.5$ represents the input variable e or e_c, i.e., $\alpha(e) = 1 - 0.6exp\left(-0.5e^2\right)$, $\alpha(e_c) = 1 - 0.6exp\left(-0.5e_c^2\right)$.

The scaling factor β of the output universe is defined by the input error e and the error rate of change ė at the same time. Based on the corresponding state of the current system, the output universe is stretched to varying degrees, and the scaling factor of the output universe is:

$$\beta(t) = K_I \sum_{i=1}^{n} p_i \int_0^t e_i(\tau)\, dt + \beta(0) \tag{27}$$

where τ is a constant, $0 < \tau < 1$, and K_I is a proportional constant, usually $\beta(0) = 1$. The scaling factor of the output universe needs to take into account the influence of K_p and K_i on the control performance. The scaling factor of the output variable K_p is consistent with the monotonicity of the error, whereas the scaling factor of the output variable K_i has a monotone inverse with the error. For this reason, the scaling factors of the output variables K_p and K_i are chosen to be $\beta_p = 2|e|$, $\beta_i = \frac{1}{|e|+0.7}$.

To sum up, the output of variable universe adaptive fuzzy control may be defined as the following:

$$y(x(t+1)) = \beta \sum_{j=1}^{m} \prod_{i=1}^{n} A_{ij}\left(\frac{x_i}{\alpha_i(t)}\right) y_j \tag{28}$$

where A_{ij} is the membership function of the fuzzy subset, x and y are the input and output of the system, x_i is the i-th input, and y_j is the j-th output. Combining the theory of variable universe and fuzzy PI control, the system state adjusts the input and output universe adaptively to make up for the shortcomings of traditional fuzzy PID control.

IV. EXPERIMENT AND RESULT

To test the effectiveness of the proposed control system in reducing tension disturbance, a simulation test is performed according to the reference values presented in Table 3 and 4. Figs. 11 (a) (b), 12 (a) (b), and 13 (a) (b) are respectively the response results of the corresponding reference tension at different start and end velocities. At t = 5 s, the unwinding section introduces speed step interference to make the tension fluctuate.

TABLE 3. Speed and tension parameters.

Case no	Reference Tension	Initial speed (rpm)	Final speed (rpm)
1	20	100	200
2	20	200	300
3	30	100	200
4	30	200	300
5	50	100	200
6	50	200	300

TABLE 4. Parameters used in simulation.

Parameter	Value	Unit
Diameter of unwind roll	0.076	m
Diameter of dancer roll	0.03	m
Circumference of rewind roll	0.857	m
Dancer swing range	-15~+15	Degree
Upstream span length	0.25	m
Downstream span length	0.6	m
Inertia of unwind roll	0.281	kg-m^2
Inertia of rewind roll	61.334	kg-m^2
Inertia of dancer system	0.2107	kg-m^2
Rod length from hinge to air cylinder	0.25	m
Rod length from hinge to dancer roll	0.27	m
Width of insulation tape	0.03	m
Young's Modulus of insulation tape	88.4615	Mpa

Through the designed variable universe fuzzy controller, ΔK_p and ΔK_i are obtained to adjust the values of K_p and K_i. Figs 11 (c) (d), 12 (c) (d), and 13 (c) (d) show that when the reference tension is 20N, 30N, 50N respectively, the initial and final speed steps to 100rpm/200rpm, K_p, and K_i are adaptively adjusted with the change of tension error. Fig 14 shows the error peak value of the corresponding reference tension at different start and end velocities.

It may be evidently observed that compared to the fixed gain PI control method, the proposed control method may effectively reduce the overshoot and undershoot of tension. In the traditional PID controller, once the speed disturbance changes from 100rpm to 200rpm, the error peak of tension increases, and when the speed changes from 200rpm to 300rpm, the tension has a larger steady-state error; also, the estimated gain of the proposed controller can compensate the change of speed quickly, improve the response speed of the system, and reduce the steady-state error. It shows better disturbance adjustment ability.

In this paper, the stability and accuracy of the control method proposed are verified by the insulation winding system shown in Fig 2, In the course of the experiment, follow these steps. First, the insulating paper tape of the unwinding roll is passed through the follower roller and the guide roller, through the dancer mechanism into the counting wheel, then through the follower roller and the guide roller; the paper tape is fixed to the spindle core mold; the air pressure is washed into the cylinder according to the tension set by the potentiometer knob; the cylinder is pushed to the limit position $-15°$ due to the relaxation pressure of the insulation belt. Secondly, the unwinding section is closed through the position loop feedback by the position sensor, the dancer returns to the reference position (the dancer arm is perpendicular to the roller and keeps at 0° position), and the tension is kept near the expected value based on which the winding work can be started. Finally, the reference speed change of the unwinding roller between the $100-300$rpm is input to evaluate the effectiveness of the system for tension and dancer position control. The only other part that controls the tension of the insulating paper tape during the test is the spindle part of the PID controller that functions in the speed ring mode. There is an initial speed ratio N between the winding spindle and the unwinder determined by the gear ratio and the diameter of the roller. The reference tension is 50N, and the experimental results are shown in Fig 15.

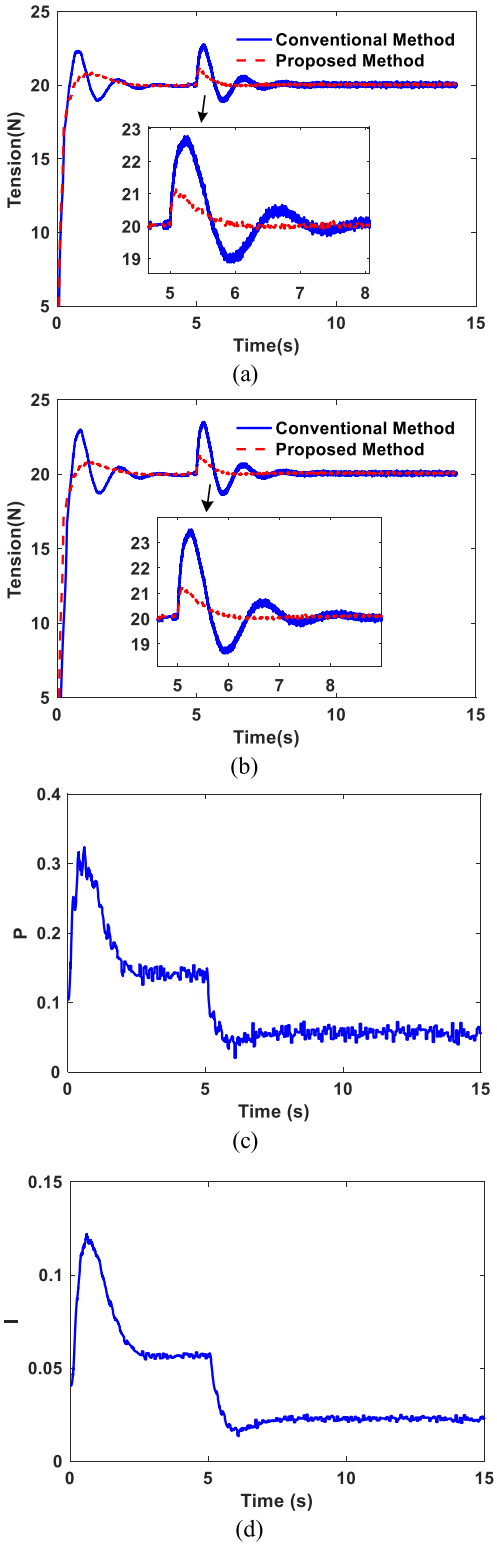

FIGURE 11. Effect of velocity step disturbance on reference tension 20N. (a) Initial speed: 100rpm, Final speed: 200rpm. (b) Initial speed: 200rpm, Final speed 300rpm. (c) Proportional gain adaptation. (d) Integral gain adaptation.

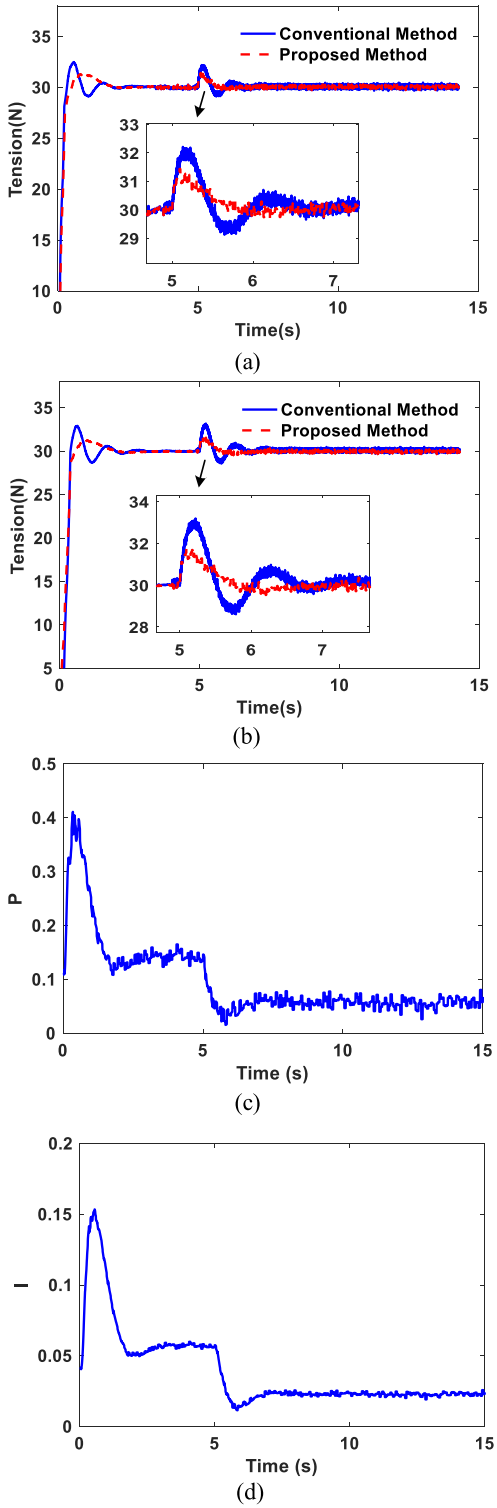

FIGURE 12. Effect of velocity step disturbance on reference tension 30N. (a) Initial speed: 100rpm, Final speed: 200rpm. (b) Initial speed: 200rpm, Final speed 300rpm. (c) Proportional gain adaptation. (d) Integral gain adaptation.

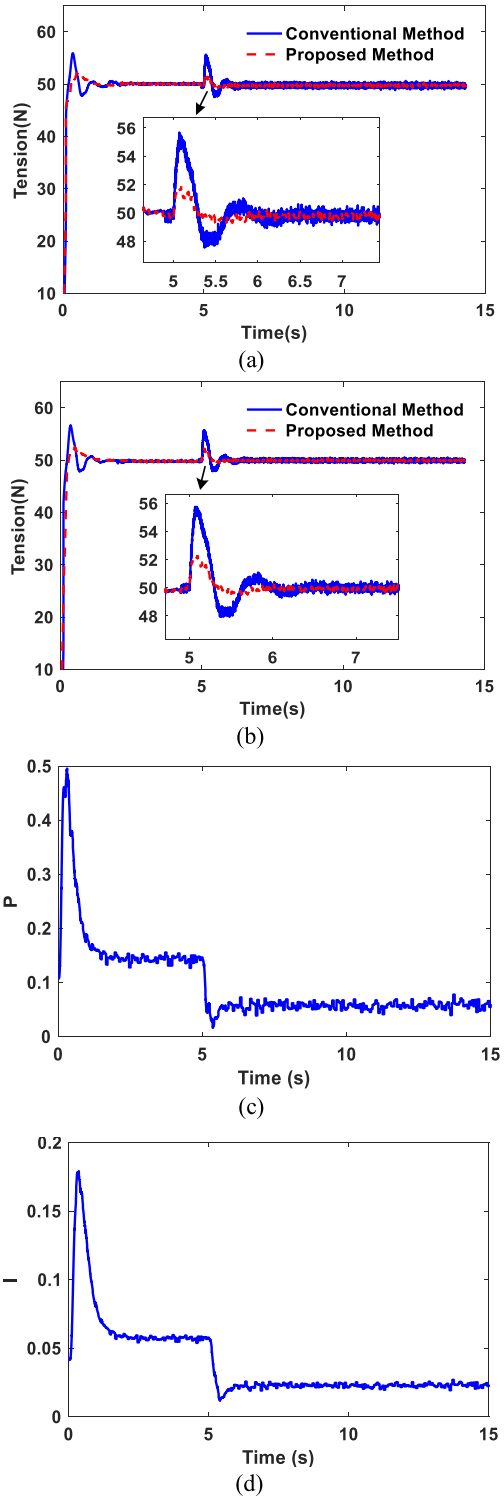

FIGURE 13. Effect of velocity step disturbance on reference tension 50N. (a) Initial speed: 100rpm, Final speed: 200rpm. (b) Initial speed: 200rpm, Final speed 300rpm. (c) Proportional gain adaptation. (d) Integral gain adaptation.

The reference value of the speed starts to increase from 0 at 20 s: it first reaches 100rpm, and the tension fluctuates between 49.7N and 51.3N; then, it increases the speed, the estimated value of gain changes continuously; later, it decreases gradually as the winding task is nearing completion, and the peak tension is 52.1N. Throughout the whole

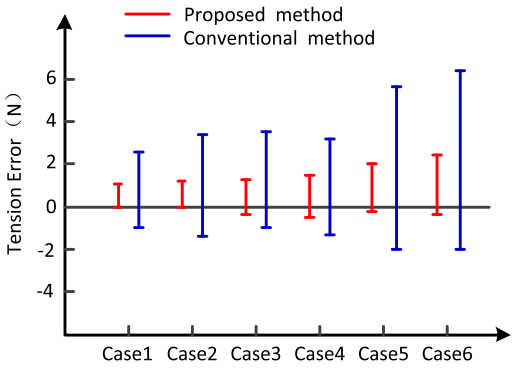

FIGURE 14. Tension error peak.

winding process, the tension fluctuates in the range of ±4% of the reference tension, and the dancer position fluctuates between −1.21° and −1.87°.

To show that the control system proposed in this paper has the better adaptive ability in insulation tape winding of elliptical iron core transformer and evaluate its effectiveness in reducing tension disturbance and steady-state error, the control method proposed, in this paper is compared with the fixed gain PI control method, and reference tension is set to 50N; the results of the position fluctuation of the dancer, as well as tension change are shown in figure 16.

The speed starts to change at 60s, and the tension under the fixed gain PI control has a great interference with the change of speed that only meets the requirement of working tension in part of the time. With the increase of speed, the precision of tension control decreases, the peak value of tension error increases with acceleration and deceleration, and the dancer float is quite strong. The tension fluctuation of the control method proposed in this article remains in a small range when the speed changes greatly. The overshoot of paper tape tension is decreased, and the system response speed is accelerated; the gain estimate is constantly adjusted with the tension error, the tension fluctuation is effectively limited to the allowable range of ±4% all through the working period, and the dancer position may be maintained in a smaller floating range.

Through experiments, it may be obtained that the tangential velocity of the insulating paper tape in the winding process of the spindle changes periodically according to the curve illustrated in Fig 17(a); the tension changes are illustrated in Fig 17(b).

Since the geometric shape of the transformer core is approximately oval, the tangent speed of the paper tape varies periodically with the radius of the mandrel throughout the winding process, causing the tension to fluctuate constantly and periodically. According to the test results at different winding speeds, it may be observed that the tension fluctuation is within the allowable range of ±4%.

Two criteria are defined to assess the performance of different controllers in order to compare and analyze the

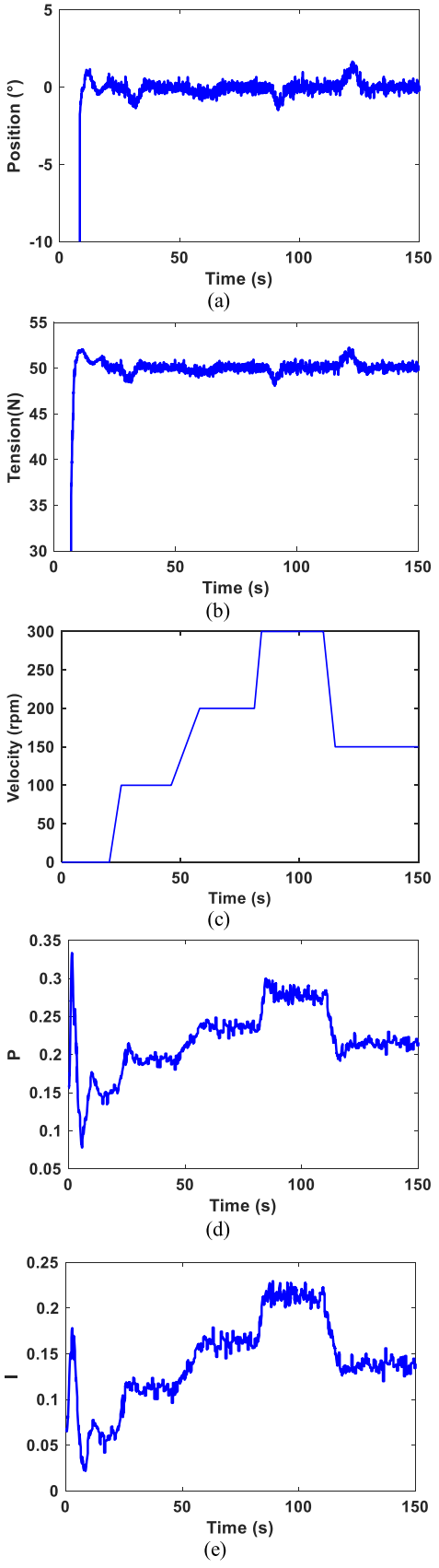

FIGURE 15. Experimental results under variable universe fuzzy PI control. (a) Dancer position. (b) Unwind tension. (c) Unwind speed. (d) Proportional gain adaptation. (e) Integral gain adaptation.

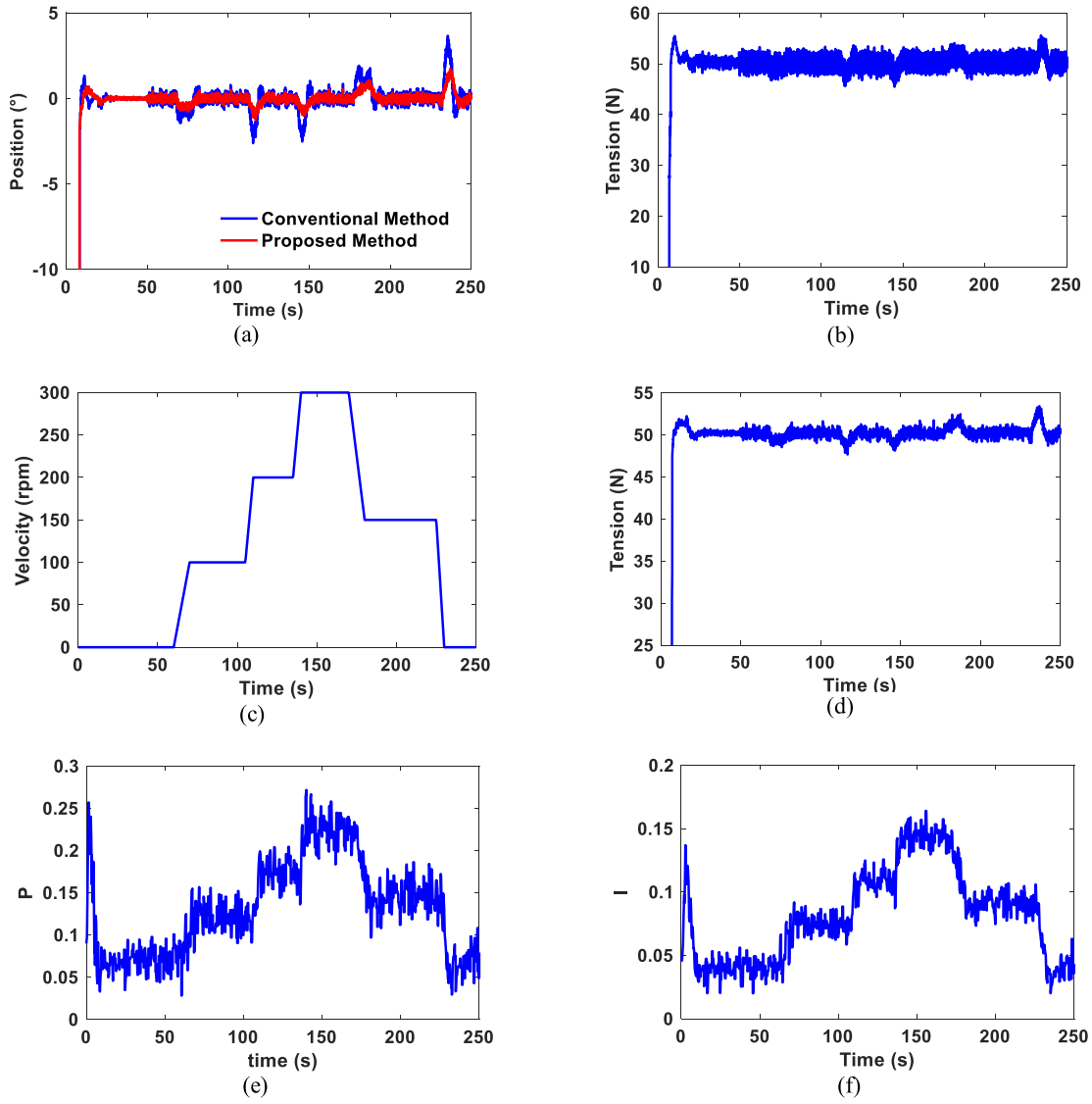

FIGURE 16. Comparison of experimental results of the fixed gain PI and variable universe fuzzy PI control. (a) Dancer position. (b) Unwind tension(PI Controller). (c) Unwind speed. (d) Unwind tension(VUF PI Controller). (e) Proportional gain adaptation. (f) Integral gain adaptation.

performance of different controllers without losing generality. The first standard is as follows:

$$H_1 = \frac{1}{T}\int_0^T \| \propto (t) - \propto_{ref} \| \, dt \tag{29}$$

Correct the absolute error standard integral that may provide the standard H_1 value per unit of time; its analysis may assess the performance and level of the system tracking reference value. The second indicator is as follows:

$$H_2 = max(\| \propto (t) - \propto_{ref} \|) \quad 0 \le t \le T \tag{30}$$

The standard is used to evaluate the extent to which the dancer deviates from the reference position, and measure the decoupling ability of the system, the influence on the dancer offset position, and tension of system when the speed changes.

TABLE 5. Controller performance comparison.

	PI controller	VUFPI controller
H_1	1.034	0.568
H_2	3.834	1.861

Table 5 shows the values of the evaluation criteria under the two control modes. Compared with fixed gain PID control, the proposed control methods in both the reference tracking performance and reduced coupling system are improved. On the contrary, under fixed gain PI control mode, the position and tension fluctuate greatly around the reference value, and the coupling between the tension and speed is obvious; however, quicker response speed can still be kept through the reasonable setting parameters. Under the control method in

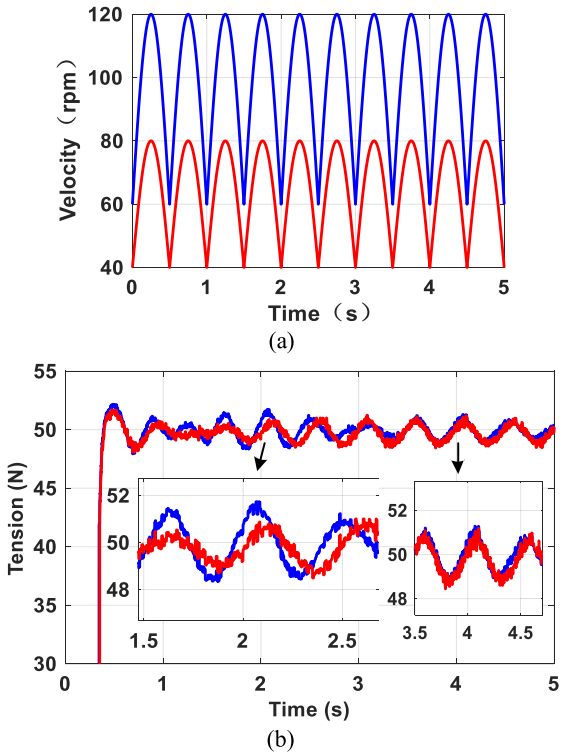

FIGURE 17. Spindle tension under variable universe fuzzy PI control. (a) Rewind speed. (b) Rewind tension (VUF PI Controller).

this article, although the fluctuation of the tension and the position of the dancer have been significantly reduced during acceleration and deceleration, a slight oscillation of position and tension in the reference attachment can be observed during steady-state operation; the main reason for these phenomena is the eccentricity and irregularity of the roller. It can also be seen that the average of the tension, in transmission and stops, is different due to the dynamic and static friction in the process of starting and stopping the driven roller; as the speed increases, the better effect. It is explained that the dynamic characteristics of driven roller affect paper tension; in the case of need higher control precision, it can be based on the driven roller friction model by adding feedforward control to provide effective compensation amount.

Generally, the traditional PID controller is applicable in industrial applications; however, for the industrial applications with fast-tracking reference signals and high control precision, it is essential to adjust the controller parameters online in order to adapt to the change of system error. Variable universe fuzzy PI control is suitable to solve this problem, and the controller parameters are adjusted in real time according to the change of error; it can well adjust and restrain the speed interference and tension fluctuation caused by the eccentricity and non-roundness of the roller. The structure of the control system based on the dancer position is simple and does not need to add a tension sensor that reduces the complexity and cost in industrial applications and meets the requirements of high tension precision. It provides a reference for the design and application of a tension control system for an insulating layer of the elliptical core transformer.

V. CONCLUSION

(1) In the unwinding section, the larger deviation of uncoiling roll radius and inertia can lead to large tension fluctuation. The larger upstream span length and its inertia in the design process of the dancer system can reduce the resonant frequency and response performance of the system.

(2) During steady-state operation, part of the tension disturbance of the winding section is caused by the time-varying characteristics of radius and inertia; however, the tangent speed of the insulating paper tape fluctuates continuously due to the periodic change of the core mold radius, resulting in periodic deviation of tension set value.

(3) In this study, a tension control system with hybrid dancer position feedback for transformer insulation winding is proposed, and a variable universe fuzzy PI controller is designed to adjust the unwinder speed. Compared with the traditional PID control method, the proposed model may effectively reduce the influence of tension disturbance in the insulation winding process of the elliptical iron core transformer. It has strong self-adaptation and anti-interference ability and can better meet the tension control requirements of the system at different winding speeds. It can solve the problems of low efficiency and poor consistency in a manual winding of transformer insulation.

REFERENCES

[1] F. S.-L. Blanc, J. Fleischer, M. Schmitt, M. Unger, and J. Hagedorn, "Analysis of wire tension control principles for highly dynamic applications in coil winding: Investigation of new tension control devices for noncicurlar orthocyclic coils," in *Proc. 5th Int. Electric Drives Prod. Conf. (EDPC)*, Sep. 2015, pp. 10–18.
[2] J. Hagedorn, F. S.-L. Blanc, and J. Fleischer, *Handbook of Coil Winding*. Berlin, Germany: Springer, 2018, pp. 11–30.
[3] H. Hui and H. Jing, "Digital design of transformer winding winding machine," *Electr. Drive*, vol. 40, no. 5, pp. 74–78, May 2010.
[4] K. M. Biggie, "Insulutions Strip-Flex K Technology for efficient distribution transformer coils," *Transf. Mag.*, vol. 4, no. 2, pp. 122–127, Mar. 2017.
[5] T. Imamura, T. Kuroiwa, K. Terashima, and H. Takemoto, "Design and tension control of filament winding system," in *Proc. IEEE Int. Conf. Syst., Man, Cybern.*, Apr. 1992, pp. 600–665.
[6] D. Kuhm and D. Knittel, "New design of robust industrial accumulators for elastic webs," *IFAC Proc. Volumes*, vol. 44, no. 1, pp. 8645–8650, Jan. 2011.
[7] J. Roppa and R. M. Govinda, "Design & implementation of closed loop PID mechanism for wire tension control (Tensioner) in winding machine," *Int. J. Instrum., Control Automat.*, vol. 1, no. 2, pp. 37–42, 2011.
[8] C. Wang, Y. Wang, R. Yang, and H. Lu, "Research on precision tension control system based on neural network," *IEEE Trans. Ind. Electron.*, vol. 51, no. 2, pp. 381–386, Apr. 2004.
[9] P. R. Raul and P. R. Pagilla, "Design and implementation of adaptive PI control schemes for Web tension control in roll-to-roll (R2R) manufacturing," *ISA Trans.*, vol. 56, pp. 276–287, May 2015.
[10] S. Liu, X. Mei, F. Kong, and K. He, "A decoupling control algorithm for unwinding tension system based on active disturbance rejection control," *Math. Problems Eng.*, vol. 2013, Nov. 2013, Art. no. 439797.
[11] V. Tu Duong, "Cross-coupling synchronous velocity control for an uncertain model of transformer winding system using model reference adaptive control method," in *Proc. Recent Adv. Electr. Eng. Rel. Sci.*, 2016, pp. 441–455.
[12] H. Kang and K.-H. Shin, "Precise tension control of a dancer with a reduced-order observer for roll-to-roll manufacturing systems," *Mech. Mach. Theory*, vol. 122, pp. 75–85, Apr. 2018.

[13] A. F. Lynch, S. A. Bortoff, and K. Röbenack, "Nonlinear tension observers for Web machines," *Automatica*, vol. 40, no. 9, pp. 1517–1524, Sep. 2004.
[14] M. A. Valenzuela, J. M. Bentley, and R. D. Lorenz, "Sensorless tension control in paper machines," *IEEE Trans. Ind. Appl.*, vol. 39, no. 2, pp. 294–304, Mar. 2003.
[15] V. Gassmann, D. Knittel, P. R. Pagilla, and M. A. Bueno, "Fixed-order H_∞ tension control in the unwinding section of a Web handling system using a pendulum dancer," *IEEE Trans. Control Syst. Technol.*, vol. 20, no. 1, pp. 173–180, Jan. 2012.
[16] D. Knittel, A. Arbogast, M. Vedrines, and P. Pagilla, "Decentralized robust control strategies with model based feedforward for elastic Web winding systems," in *Proc. Amer. Control Conf.*, 2006, pp. 1968–1975.
[17] P. R. Raul, S. G. Manyam, P. R. Pagilla, and S. Darbha, "Web tension regulation with partially known periodic disturbances in roll-to-roll manufacturing systems," in *Proc. Eur. Control Conf. (ECC)*, Jul. 2015, pp. 1089–1098.
[18] H. Kang, C. Lee, and K. Shin, "Modeling and compensation of the machine directional register in roll-to-roll printing," *Control Eng. Pract.*, vol. 21, no. 5, pp. 645–654, May 2013.
[19] R. V. Dwivedula, Y. Zhu, and P. R. Pagilla, "Characteristics of active and passive dancers: A comparative study," *Control Eng. Pract.*, vol. 14, no. 4, pp. 409–423, Apr. 2006.
[20] Z. F. Qing, D. Huang, W. H. Gui, and C. H. Yang, "Research and application of interpolation fuzzy PID control system based on variable universe," *Chin. J. Sci. Instrum.*, vol. 29, no. 11, pp. 2435–2440, Nov. 2008.
[21] H. Zheng, H. B. Xu, and G. P. Zhu, "Application of variable universe adaptive fuzzy control in aircraft power generation," *Control Theory Appl.*, vol. 25, no. 2, pp. 253–256, Apr. 2008.
[22] G. Ponniah, M. Zubair, Y.-H. Doh, and K.-H. Choi, "Fuzzy decoupling to reduce propagation of tension disturbances in roll-to-roll system," *Int. J. Adv. Manuf. Technol.*, vol. 71, nos. 1–4, pp. 153–163, Mar. 2014.

HAIXIANG HUANG received the B.S. degree in electrical engineering and automation from the Harbin University of Science and Technology, Harbin, China, in 2018, where he is currently pursuing the M.S. degree with the Automation School.

His research interests include industrial control automation and production process automation.

JIAZHONG XU received the B.S. and M.S. degrees in mechanical engineering from Northeast Agricultural University, Harbin, China, in 1999 and 2002, respectively, and the Ph.D. degree in mechanical design manufacturing and automation from the Harbin University of Science and Technology, Harbin, in 2007.

He is currently the Dean of the Automation School, Harbin University of Science and Technology. His research interests include mechatronics and robotics.

KEWEI SUN received the B.S. and M.S. degrees in biomedical engineering from Yanshan University, Qinhuangdao, China, in 2008 and 2011, respectively. He is currently pursuing the Ph.D. degree in mechanical and power engineering with the Automation School, Harbin University of Science and Technology.

His research interests include intelligent equipment manufacturing, instrumentation, and medical equipment.

LIWEI DENG received the M.S. degree from the Harbin University of Science and Technology, Harbin, China, in 2010, and the Ph.D. degree from the Harbin Institute of Technology, Harbin, in 2014.

He is currently an Associate Professor with the Harbin University of Science and Technology. His research interests include control science and engineering, fractional order systems, digital imaging processing, and deep learning algorithm.

CHENG HUANG received the Ph.D. degree in control science and engineering from the Harbin Institute of Technology, Harbin, China, in 2018.

He is currently a Lecturer with the School of Automation, Harbin University of Science and Technology. His main research interests include spacecraft rendezvous, docking control, and nonlinear control.